Open access • Journal Article • DOI:10.1103/PHYSREVLETT.101.064503

Massive amplification of surface-induced transport at superhydrophobic surfaces.

David M. Huang, Cécile Cottin-Bizonne, Christophe Ybert, Lydéric Bocquet ...+1 more authors

Institutions: University of Lyon, Technische Universität München

Published on: 08 Aug 2008 - Physical Review Letters (American Physical Society)

Topics: Marangoni effect and Slip (materials science)

Massive Amplification of Surface-Induced Transport at Superhydrophobic Surfaces

David M. Huang,[1,*] Cécile Cottin-Bizonne,[1] Christophe Ybert,[1] and Lydéric Bocquet[1,2]

[1]*LPMCN, Université de Lyon, Université Lyon 1 and CNRS, UMR 5586, F-69622 Villeurbanne, France*

[2]*Physics Department, Technical University Munich, 85748 Garching, Germany*

(Received 16 May 2008; published 8 August 2008)

We study electro- and diffusio-osmosis of aqueous electrolytes at superhydrophobic surfaces by means of computer simulation and hydrodynamic theory. We demonstrate that the diffusio-osmotic flow at superhydrophobic surfaces can be amplified by more than 3 orders of magnitude relative to flow in channels with a zero interfacial slip. By contrast, little enhancement is observed at these surfaces for electro-osmotic flow. This amplification for diffusio-osmosis is due to the combined effects of enhanced slip and ion surface depletion or excess at the air-water interfaces on superhydrophobic surfaces. This effect is interpreted in terms of capillary driven Marangoni motion. A practical microfluidic pumping device is sketched on the basis of the slip-enhanced diffusio-osmosis at a superhydrophobic surface.

DOI: 10.1103/PhysRevLett.101.064503 PACS numbers: 47.61.−k, 47.10.ad, 68.15.+e, 82.39.Wj

The recent development of artificial superhydrophobic (SH) surfaces has opened a whole new field of investigation, with both fundamental and practical perspectives [1,2]. Such SH surfaces are able to trap air at the liquid-solid interface, leading to their exceptional nonwetting properties, with a very high water contact angle—close to 180°—and low hysteresis. This strong hydrophobicity has remarkable implications in the context of self-cleaning [2] and impact processes [1,3]. But in addition to water repellency, the peculiar fluid dynamics close to SH surfaces is also particularly promising, with potential applications in microfluidics [4,5]. Recent studies have demonstrated the drag-reducing ability of SH surfaces [6–8] associated with large slippage of the fluid at SH surfaces. Slippage is usually quantified by the slip length b [defined by $\mathbf{v}(z=0) \equiv b\,\frac{\partial \mathbf{v}}{\partial z}|_{z=0}$, where $\mathbf{v}$ is the interfacial velocity] [9]: on SH surfaces, the (effective) slip length b_{eff} can reach microns, several orders of magnitude larger than on smooth hydrophobic surfaces [10,11].

Besides this drag-reduction potential in pressure-driven flows, it has recently been predicted that slippage could be best exploited in surface-driven transport [12,13], such as electro-osmosis (EO)—flow induced by electric potential gradients—and diffusio-osmosis (DO)—flow induced by solute concentration gradients [14]. For such transport processes, a large slip-induced flow amplification that scales like $(1 + b/\lambda)$ may be achieved, with λ typically the nanometric Debye layer width: near a smooth uniform surface with $b \sim 20$–30 nm [10,11], an order of magnitude enhancement is typically expected. As recently discussed [15], such slip-induced amplifications are particularly relevant in the context of electrical energy conversion.

Now, combining these ideas would suggest that a massive amplification can be reached for surface-induced transport on SH surfaces. Such an effect, potentially of order $b_{\mathrm{eff}}/\lambda \sim 10^2$–$10^4$, would provide extremely efficient microfluidic pumping based on electrical (EO) or chemical (DO) transduction. However, the answer to this question is by no means obvious, since the slip length on SH surface (denoted b_{eff}) is an effective one, defined from the far-field hydrodynamic behavior: it thus results from the complex flow pattern at a scale $L \gg \lambda$ characterizing the surface roughness of the SH surface.

In this Letter, we show (i) that massive amplification of surface-driven transport can indeed be achieved in experimentally realizable microfluidic channels with SH surfaces, but (ii) that the amplification depends on the transport process considered: no amplification is obtained for EO on SH surfaces, while an amplification of more than 3 orders of magnitude can be achieved for DO. These conclusions are supported by molecular dynamics simulations and a continuum model that combines continuum hydrodynamics and a modified Poisson-Boltzmann description for the interfacial ion densities.

In what follows, we will explicitly focus on EO and DO, with a salt as the solute. DO has caught less attention than EO for flow generation but, as we will argue, it provides in addition to slip-induced flow amplification the advantage of permitting ''source-free'' microfluidics, in which the flow is generated by the constituents of the fluid, rather than requiring an external input of electrical energy, such as an electric source in the case of EO.

Before turning to the numerical calculations, let us first present a simple physical argument to estimate the enhancement of surface-driven transport at a composite SH interface. For any interfacially driven mechanism, motion occurs through a global balance between the (laterally averaged) interfacial driving force $\langle F_{\mathrm{drive}}\rangle$, which occurs within the interfacial layer of thickness λ, and the (viscous) friction force $\langle F_{\mathrm{friction}}\rangle$. For a SH surface, characterized by a slip length $b_{\mathrm{eff}} \gg \lambda$, $\langle F_{\mathrm{friction}}\rangle = \eta\langle v_{\mathrm{slip}}\rangle/b_{\mathrm{eff}}$, where $\langle v_{\mathrm{slip}}\rangle$ is the laterally averaged slip velocity at the surface and η is the fluid viscosity. If F_{drive} is approximately homogeneously distributed over the surface, then $\langle F_{\mathrm{drive}}\rangle \approx \eta(\langle v_s\rangle - \langle v_{\mathrm{slip}}\rangle)/\lambda$, where $\langle v_s\rangle$ is the averaged velocity outside the interfacial region. Equating $\langle F_{\mathrm{drive}}\rangle$ and $\langle F_{\mathrm{friction}}\rangle$ gives

$$v_s \approx \frac{\lambda}{\eta}\langle F_{\text{drive}}\rangle\left[1+\frac{b_{\text{eff}}}{\lambda}\right]. \quad (1)$$

Now, the key point is the lateral distribution of driving forces, F_{drive}. In EO, the electric force (integrated over the interface width) is $F_{\text{drive}} = eE\int dz(c_+ - c_-)$, where E is the applied electric field, e is the elementary charge, and $c_\pm$ are the concentrations of the positive and negative ions. Therefore, F_{drive} vanishes near the charge-neutral air-water interfaces present at SH surfaces, and flow is only generated over the solid regions: the benefit of b_{eff} is lost by the decrease of the driving force, and no amplification is expected for EO, in agreement with a recent analysis [16]. On the other hand, for DO, the local driving force is the osmotic pressure gradient within the interface and $F_{\text{drive}} = -k_BT\Gamma\nabla\ln c_0$, with $\Gamma \equiv \int dz(c_+ + c_- - 2c_0)$ the surface excess, where c_0 is the electrolyte concentration far from the interface [13]. The key point is that, due to the interactions of ions with the air-water interface (e.g., image charge repulsion or specific adsorption), Γ does not vanish over the dominant air-water interface at the SH surface, and F_{drive} is approximately uniformly distributed. Consequently, a flow amplification of $(1 + b_{\text{eff}}/\lambda)$ is indeed expected for DO.

We note finally that the expression in Eq. (1) for the DO velocity can be reexpressed in a more transparent form. Indeed, using Gibbs adsorption equation, the surface excess Γ can be rewritten in terms of the air-water surface tension γ_{LV} as $\Gamma = -\frac{1}{k_BT}[\frac{\partial\gamma_{\text{LV}}}{\partial\ln c_0}]$. Assuming $b_{\text{eff}} \gg \lambda$, Eq. (1) thus takes the form

$$v_s \approx \frac{b_{\text{eff}}}{\eta}\frac{\partial\gamma_{\text{LV}}}{\partial c_0}\nabla c_0. \quad (2)$$

This equation is similar to Young's equation for Marangoni motion [14], with the slip length replacing the droplet size. This expression highlights the physical mechanism at hand and shows that in the SH limit, DO is fully equivalent to Marangoni driving.

We now turn to the validation of this simple analysis using molecular dynamics (MD) simulations. We will define EO and DO mobilities, $\tilde{\mu}_{\text{EO}}$ and μ_{DO}, according to $v_{\text{EO}} \equiv -\tilde{\mu}_{\text{EO}}(\frac{eE}{k_BT})$ and $v_{\text{DO}} \equiv \mu_{\text{DO}}\nabla\ln c_0$, with v_{EO} and v_{DO} the EO and DO velocities outside the interfacial region. For surfaces without slip, one has roughly $\tilde{\mu}_{\text{EO}} \sim \mu_{\text{DO}} \sim \mu_0$, with $\mu_0 \equiv \frac{k_BT}{2\pi\eta l_B}$ [14] [$l_B \equiv e^2/(4\pi\epsilon_0\epsilon_w k_BT)$, the Bjerrum length]. MD simulations of EO and DO were carried out on systems consisting of an aqueous electrolyte ([NaCl] or [NaI] $\approx$ 1 M) confined between parallel solid walls. The simulation model and parameters used were identical to those described in Ref. [17] except that both smooth hydrophobic and SH surfaces were studied. A snapshot of one of the simulated systems is depicted in Fig. 1, showing the solid ridges extending parallel to the y axis. Charged surfaces of uniform charge density Σ were modeled by adding identical charges to each of the atoms in the top solid layer in contact with the fluid (i.e., only on top of the ridges for the SH surfaces). Simulations were carried out in the NVT ensemble at a temperature T of 298 K and an average pressure of 1 atm. In the EO simulations, flow was induced by applying an electric field E in the x direction to each charged fluid atom. DO was measured indirectly in pressure-driven flows by the method in Ref. [13], yielding the DO mobility using $\mu_{\text{DO}} \equiv -\frac{k_BT}{H}(\frac{J-2c_0Q}{-\nabla p})$, where $J = J_+ + J_-$ is the total solute current of positive and negative ions, Q the total flow rate, and c_0 the bulk salt concentration (measured in the center of the simulation cell). The pressure gradient, $\nabla p \approx -f_x\rho_f$, was simulated by applying a uniform force f_x in the x direction to each fluid atom (ρ_f is the bulk density of fluid atoms). Linear response of the system to the applied force was verified in all simulations. MD results for the DO and EO mobilities, μ_{DO} and $\tilde{\mu}_{\text{EO}}$, are shown in Fig. 2 as functions of the surface solid fraction $\phi_s = a/L$. First, these simulations confirm qualitatively the previous simple analysis: an amplification of the DO mobility is measured as the solid fraction decreases ($\phi_s \to 0$, SH limit), whereas no such amplification is observed for the EO mobility (inset). Going into more detail, we also observe a very strong ion-specific effect for DO, since the mobilities for NaI and NaCl salts are of opposite sign: the flow is towards less salt for NaI and vice versa for NaCl. This behavior is due to the ion-specific enhancement of NaI near neutral hydrophobic and air-water interfaces [17,18], which contrasts with the depletion of NaCl near the same interfaces. The depletion of NaCl is a manifestation of the importance of the image-charge repulsion for this salt at all concentrations. This correlates moreover with the sign of $\frac{\partial\gamma_{\text{LV}}}{\partial c_0}$ for these two salts in simulations [18], as expected according to Eq. (2). This result demonstrates the interesting possibility of controlling both the flow magnitude and direction in DO by altering the electrolyte type.

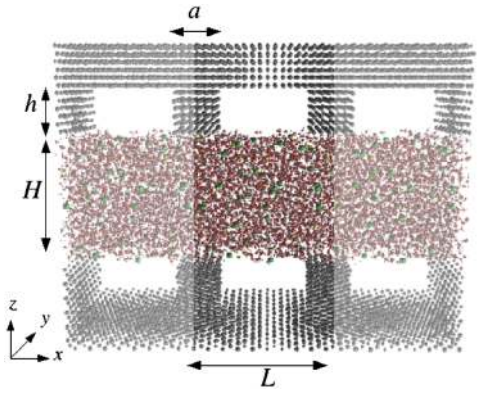

FIG. 1 (color online). Snapshot of one of the simulated systems, depicting the primary simulation cell and two periodic replicas in the x-direction (lighter shading). The period of the system is L, the distance between closest sections of opposite walls is H, and the width and height of the bumps are a and h, respectively. In all simulations, we used $h = 3\ell_{\text{sp}}$, $a = 3\ell_{\text{sp}}$, with $\ell_{\text{sp}} = 5.357$ Å the lattice spacing.

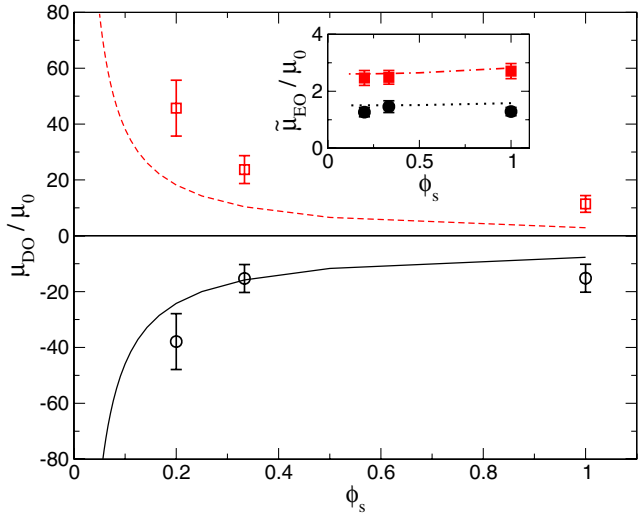

FIG. 2 (color online). Normalized DO mobility μ_{DO}/μ_0, where $\mu_0 \equiv k_B T/(2\pi\eta l_B)$, from computer simulations (NaI: ○; NaCl: □) and continuum hydrodynamics calculations (NaI: solid line; NaCl: dashed line) as a function of solid fraction $\phi_s = a/L$ for neutral surfaces. For the continuum calculations, we used $\epsilon_w = 68$ [25] and $b_s = 55$ Å [17], obtained from independent equilibrium and Couette flow simulations of SPC/E water under similar thermodynamic conditions. Inset: EO mobility $\tilde{\mu}_{EO}/\mu_0$ from simulations (NaI: ●; NaCl: ■) and continuum hydrodynamics calculation (NaI: dotted line; NaCl: dash-dotted line) for $\Sigma = +0.062$ C/m^2.

We now propose a continuum hydrodynamic model, which aims to bridge the gap between the nanoscales involved in MD simulations and the microscales characterizing real SH surfaces, while capturing the subtle ion-specific effects observed in MD. The model involves the Stokes equation for the fluid flow and a modified Poisson-Boltzmann (PB) formulation for the ions distribution. The latter formulation, based on our previous work in Ref. [17], allows the ion-specific distributions at hydrophobic and air-water interfaces to be captured. While the validity of such a mean-field approach is *a priori* restricted to low salt concentration, it captures the main physical mechanisms and provides good semi-quantitative predictions [17]. We write the Stokes equation as

$$-\eta\nabla^2\mathbf{v} + \nabla\delta p \simeq f_{\text{drive}}, \tag{3}$$

where $\delta p = p - \pi$ is the difference between the total pressure p and the local osmotic pressure, $\pi = k_B T(c_+ + c_- - 2c_0)$. This equation was derived assuming that the fluid structure was decoupled from the dynamics, such that the ion density distributions $c_\pm$ could be described by thermal equilibrium $c_\pm(x, y, z) = c_0(x) \times \exp[-U_\pm(x, y, z)/k_B T]$. Assuming 1:1 electrolytes and identical diffusion constants for the positive and negative ions, $f_{\text{drive}} = -k_B T(c_+ + c_- - 2c_0)\nabla \ln c_0$ for DO and $e(c_+ - c_-)E$ for EO [14]. Slip boundary conditions were applied at the boundary at $z = 0$ representing the solid-liquid and vapor-liquid interfaces of the SH surface: $b(x, y)\partial_z v_{x,y}|_{z=0} = v_{x,y}|_{z=0}$ (b finite) or $\partial_z v_{x,y}|_{z=0} = 0$ ($b \to \infty$). Two slip patterns were considered: (i) solid square posts of side-length a evenly spaced by a distance L and (ii) solid ridges of width a parallel to the y axis and evenly spaced by a distance L, in both cases with slip length b_s and separated by regions of infinite slip. For the ion density distributions, we generalized our modified PB formulation from Ref. [17] to a system with patterned solute-surface interactions: $c_\pm(x, y, z) = c_0 \exp\{-[\pm eV(\mathbf{r}) + U^\pm_{\text{ext}}(\mathbf{r})]/k_B T\}$, where the electrostatic potential V is computed self-consistently from the Poisson equation $\Delta V = -e[c_+(x, y, z) - c_-(x, y, z)]/\epsilon_w\epsilon_0$. In this modified PB equation, $U^\pm_{\text{ext}}$ is the external potential acting on the ions due to interactions other than the electrical potential V: this includes the solid-fluid Lennard-Jones (LJ) interaction, $U^\pm_{\text{wall}}$, an ion-size-dependent hydrophobic solvation energy, $U^\pm_{\text{hyd}}$ [17], and the image-charge repulsion, $U^\pm_{\text{im}}$ [19]. The continuum equations were then solved with the COMSOL finite-element software for a slit pore that was periodic in the x and y directions and had a plane of reflection symmetry at $z = H/2$, the channel center. The DO or EO velocity v_s was defined as the midchannel fluid velocity $v_x(x, y, z = H/2)$ averaged over x and y.

Predictions for the mobilities are compared with the MD simulations in Fig. 2. A first important point is that the model indeed captures the amplification effect for DO, and its absence for EO. Furthermore, the modified PB model is able to reproduce the subtle ion-specific effects observed in MD, which originates from iodide enhancement and chlor-

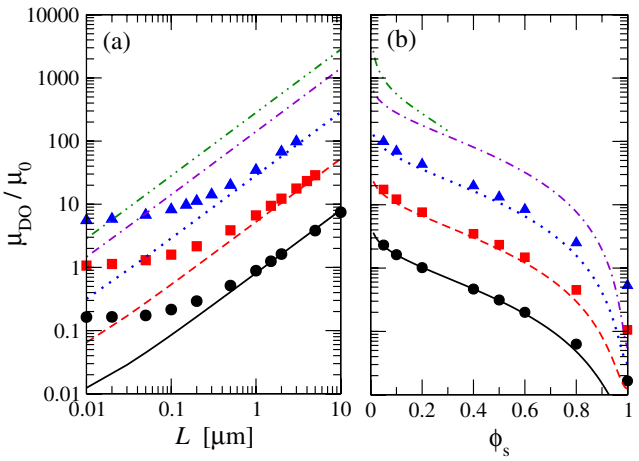

FIG. 3 (color online). Normalized DO mobility μ_{DO}/μ_0 as a function of (a) periodicity L for a fixed solid fraction $\phi_s = 0.1$ and (b) solid fraction ϕ_s for a fixed periodicity $L = 2$ μm, from continuum hydrodynamics calculations of systems with solid ridges for [NaCl] = 0.001 M (●), 0.01 M (■), and 0.1 M (▲) (with $b_s = 55$ Å on the solid surfaces). The lines are the predictions using Eq. (1) for solid ridges with (from bottom to top) [NaCl] = 0.001 M, 0.01 M, 0.1 M, and 1.0 M; and for solid posts with [NaCl] = 1.0 M (top curve). The interface width λ was obtained from the predicted ion profile on the liquid-vapor interface [20]. Experimental values for $\eta = 0.890$ mPa s and $\epsilon_w = 77.8$ of pure liquid water at ambient conditions were used.

ide depletion at the vapor-liquid interfaces. Altogether, an overall good agreement is found, thus supporting the general picture proposed by the model. Finally, let us note that, while the agreement is only semi-quantitative for DO, it is expected to improve with decreasing salt concentration, for which long-range electrostatic interactions dominate and errors due to the simple form used for $U^{\pm}_{\mathrm{ext}}$ become less relevant.

On the basis of the proposed framework, we extended the continuum calculations to treat lower salt concentrations and values of L more relevant to experimental SH surfaces. The DO mobility μ_{DO}, calculated with our continuum model for [NaCl] with various molarities, is shown in Fig. 3 for uncharged SH surfaces with varying roughness characteristics. We now compare these results with the expected amplification factor $[1 + b_{\mathrm{eff}}(\phi_s)/\lambda]$ in Eq. (1) [20]. For a SH surface made of ridges, the expression for $b_{\mathrm{eff}}(\phi_s)$ has been obtained previously [21]: $b_{\mathrm{eff}}(\phi_s) = -\frac{L}{2\pi}\ln\{\cos[(1-\phi_s)\frac{\pi}{2}]\} \equiv b_\perp$ (for flow perpendicular to the ridges). For a SH surface made of solid posts, $b_{\mathrm{eff}} \approx L(0.325/\sqrt{\phi_s} - 0.44)$ (for $\phi_s \lesssim 0.3$) [22]. The predictions of Eq. (1) with the amplification factor of the mobility, $[1 + b_{\mathrm{eff}}(\phi_s)/\lambda]$, are compared in Fig. 3 with the continuum results. A very good agreement is found in the SH limit, i.e., small solid fraction ϕ_s (large L). Deviations are observed as expected at larger ϕ_s (smaller L), since the scale separation on which Eq. (1) relies implicitly is not effective anymore. Note that a similarly good agreement was obtained for the SH surfaces with an array of solid square posts (not shown). From Fig. 3, it can be seen that DO flow can be enhanced by 3 orders of magnitude relative to the no-slip case (for which $\mu_{\mathrm{DO}} \approx \mu_0$). The enhancement is even greater for a surface with solid square posts, as shown in Fig. 3.

To conclude, we discuss a practical realization exploiting the massive amplification of DO transport for efficient microfluidic pumping. We consider accordingly a microfluidic channel composed of one SH wall and three nonslipping walls. A concentration gradient of salt perpendicular to the main axis of the channel is built up by making the two facing nonslipping walls out of a gel permeable to salt as proposed in Ref. [23]. The SH surface pattern is striped and makes an angle θ with the main axis so that a velocity perpendicular to the main axis would result in a helical flow, with a total flow rate in the direction of the channel axis. An analytical estimate for the flow generated by the effective DO velocity near the SH surface can be obtained in the limit of a channel width w much larger than the height H, following the procedure in Ref. [24]. The total flow rate in the direction of the channel axis is $J \approx \frac{Hw}{2}(v_\perp \sin\theta + v_\parallel \cos\theta)$, with $v_\perp = \mu_\perp \hat{x}_1 \cdot \nabla \ln c$ and $v_\parallel = \mu_\parallel \hat{y}_1 \cdot \nabla \ln c$, where $\hat{x}_1$ and $\hat{y}_1$ are units vectors perpendicular and parallel to the SH stripes, respectively. Here, $\mu_{\perp,\parallel} \equiv -\frac{k_B T}{\eta}\Gamma\lambda(1 + b_{\perp,\parallel}/\lambda)$ and $b_\parallel = 2b_\perp$ [21]. Using realistic values, $w = 50\ \mu$m, $\theta = 45°$, a variation of the concentration of the salt across the channel of 1.0 M ($\nabla \ln c = 20\ \mathrm{mm}^{-1}$) and an experimentally feasible SH surface with $L = 5\ \mu$m and $\phi_s = 0.1$ [1], the average flow velocity in this case could reach 2 mm/s (using the results from Fig. 3). For comparison, to achieve the same velocity in EO for a surface with $\zeta = 100$ mV and zero slip, a substantial applied electric field of around 10^3 V/cm would be necessary.

In conclusion, we have demonstrated a massive amplification of diffusio-osmotic flow in experimentally realizable superhydrophobic channels. These results illustrate the possibility of a novel and efficient method for microfluidic pumping using chemical transduction as the driving power.

This work was supported by ANR PNANO. L. B. acknowledges support from the von Humboldt Foundation.

*Current address: Chemical Engineering and Materials Science Department, University of California, Davis, Davis, CA 95616, USA.

[1] M. Callies and D. Quéré, Soft Matter **1**, 55 (2005).
[2] R. Blossey, Nature Mater. **2**, 301 (2003).
[3] C. Duez *et al.* Nature Phys. **3**, 180 (2007).
[4] T. M. Squires and S. R. Quake, Rev. Mod. Phys. **77**, 977 (2005).
[5] J. Eijkel, Lab Chip **7**, 299 (2007).
[6] J. Ou, B. Perot, and J. P. Rothstein, Phys. Fluids **16**, 4635 (2004).
[7] C.-H. Choi and C.-J. Kim, Phys. Rev. Lett. **96**, 066001 (2006); P. Joseph *et al.*, *ibid.* **97**, 156104 (2006).
[8] L. Bocquet and J.-L. Barrat, Soft Matter **3**, 685 (2007).
[9] O. I. Vinogradova, Int. J. Miner. Process. **56**, 31 (1999).
[10] C.-H. Choi, K. J. A. Westin, and K. S. Breuer, Phys. Fluids **15**, 2897 (2003).
[11] C. Cottin-Bizonne *et al.*, Phys. Rev. Lett. **94**, 056102 (2005).
[12] V. M. Muller *et al.*, Colloid J. USSR **48**, 606 (1986).
[13] A. Ajdari and L. Bocquet, Phys. Rev. Lett. **96**, 186102 (2006); L. Joly *et al.*, *ibid.* **93**, 257805 (2004).
[14] J. L. Anderson, Annu. Rev. Fluid Mech. **21**, 61 (1989).
[15] Y. Ren and D. Stein, Nanotechnology **19**, 195707 (2008).
[16] T. M. Squires, report [Phys. Fluids (to be published)].
[17] D. M. Huang *et al.*, Phys. Rev. Lett. **98**, 177801 (2007).
[18] D. Horinek and R. R. Netz, Phys. Rev. Lett. **99**, 226104 (2007).
[19] M. Manciu and E. Ruckenstein, Adv. Colloid Interface Sci. **105**, 63 (2003).
[20] We define $\lambda = \int dz z(c_+ + c_- - 2c_0)/\int dz(c_+ + c_- - 2c_0)$.
[21] E. Lauga and H. A. Stone, J. Fluid Mech. **489**, 55 (2003).
[22] C. Ybert *et al.*, Phys. Fluids **19**, 123601 (2007).
[23] J. Diao *et al.*, Lab Chip **6**, 381 (2006).
[24] A. D. Stroock *et al.*, Anal. Chem. **74**, 5306 (2002).
[25] P. Höchtl *et al.*, J. Chem. Phys. **109**, 4927 (1998).